

## X-ray Determination of Crystallinity and Diffuse Disorder Scattering

BY W. RULAND

*European Research Associates, s. a., 95, rue Gatti de Gamond, Brussels 18, Belgium*

(Received 11 January 1961)

An X-ray method of crystallinity determination has been developed which takes into account the diffuse scattering due to thermal vibrations and lattice imperfections in the crystalline part of a substance. Application of the method to a series of polypropylene samples shows that this diffuse scattering is predominantly caused by thermal motions.

The normalization of the scattering curve leads to special absorption corrections for Compton scattering and indicates a scattering effect attributed to the carbon-hydrogen bond orbital.

### Introduction

The characteristic differences in the X-ray diffraction of crystalline and amorphous substances have led to methods (Goppel & Arlmann, 1949; Kast & Flaschner, 1948; Matthews, Peiser & Richards, 1949; Hermans & Weidinger, 1950; Krimm & Tobolsky, 1951; Aggarwal & Tilley, 1955) which use the intensity relations between the 'crystalline peaks' and the 'amorphous background' or the absolute intensity of one of these to determine the relative amounts of crystalline and amorphous material. These methods imply that the intensity of the 'crystalline peaks' and the 'amorphous background' can be unambiguously correlated with the weight fractions of crystalline and amorphous material. However, even an entirely crystalline substance shows diffuse coherent scattering and a loss in intensity of the diffraction peaks due to thermal vibrations of the atoms as well as to lattice imperfections, effects which have been emphasized in a recent paper by Hosemann *et al.* (1960). A correct method of crystallinity determination should take these effects into account.

### Theoretical

Let us consider a substance containing a weight fraction  $x_{cr}$  of crystalline material, the crystallites being ideally imperfect and large enough for their diffraction peaks to be separated without difficulty from the diffuse scattering. The amorphous fraction should have the same chemical composition as the crystalline one. Let  $I$  be the total coherent scattering of this substance measured in electron units, normalized to the average scattering per atom.  $I(\mathbf{s})$  is the value of  $I$  at the end of the reciprocal space vector  $\mathbf{s} = (\mathbf{S} - \mathbf{S}_0)/\lambda$ ;  $|\mathbf{s}| = s = (2/\lambda) \sin \theta$ . Let  $I_{cr}$  be the part of the coherent scattering which is concentrated into the diffraction peaks. Following Kartha (1953) and Norman (1957), integration over the whole of reciprocal space leads to the following expressions

$$\int_0^\infty I(\mathbf{s}) dv_s = 4\pi \int_0^\infty s^2 I(s) ds = 4\pi \int_0^\infty s^2 \overline{f^2} ds, \quad (1)$$

$dv_s$ : volume element in reciprocal space,

$\overline{f^2}$ :  $\sum N_i f_i^2 / \sum N_i$ ,

$f_i$ : scattering factor of an atom of type  $i$ ,

$N_i$ : number of atoms of type  $i$ ,

$$I(s) = \frac{1}{4\pi} \int_0^{4\pi} I(\mathbf{s}) d\omega, \quad (2)$$

$\omega$ : solid angle in reciprocal space.

$$\begin{aligned} \int_0^\infty I_{cr}(\mathbf{s}) dv_s &= 4\pi \int_0^\infty s^2 I_{cr} ds = x_{cr} / (NV) \sum_h \sum_k \sum_l |F_{hkl}^2| \\ &= x_{cr} 4\pi \int_0^\infty s^2 \overline{f^2} D ds, \end{aligned} \quad (3)$$

$V$ : volume of the unit cell,

$N$ : number of atoms in the unit cell,

$F_D$ : structure factors taking into account deviations of the atoms from their ideal positions,

$D$ : 'disorder' function.

For substances without orientation either in the crystalline or in the non-crystalline part,  $I(s)$  and  $I_{cr}(s)$  are obtained by appropriate Debye-Scherrer techniques; for oriented samples, randomization in the sense of equation (2) must be performed.

The 'disorder' function  $D(s)$  takes into account the loss of intensity concentrated at the reciprocal-lattice points due to deviations of the atoms from their ideal positions. These deviations may be due to thermal vibrations and lattice imperfections of the first kind (in which the long-range order is conserved) and of the second kind (in which the long-range order is destroyed, 'paracrystal').

Equations (1) and (3) give:

$$\mu_{cr} = \frac{\int_0^\infty s^2 I_{cr} ds}{\int_0^\infty s^2 I ds} = \frac{\int_0^\infty s^2 \overline{f^2} ds}{\int_0^\infty s^2 \overline{f^2} D ds}. \quad (4)$$

If only thermal motion is involved the  $D$ -function is identical with an isotropic Debye-Waller factor. For lattice imperfections of the first kind,  $D$  will also be gaussian, whereas for lattice imperfections of the second kind  $D$  will be approximately a function of the type  $2 \exp(-as^2)/[1 + \exp(-as^2)]$  (Hosemann, 1950, 1951), but since the imperfections of the second kind produce increasing peak broadening with increasing values of  $s$ , there is a tendency for the peaks to disappear more rapidly by their overlap.

To a first approximation  $D$  may thus be taken as  $\exp(-ks^2)$ , where  $k$  includes the effect of thermal motion as well as lattice imperfections in general.

It should, however, be emphasized that equations (3) and (4) are not valid when the disorder effects are strongly anisotropic. If, for example, only  $hk0$  or  $00l$  peaks appear sharply in  $s^2I(s)$ , due to such effects equation (3) becomes

$$\int_0^\infty I_{cr}(\mathbf{s}) dv_s = 4\pi \int_0^\infty s^2 I_{cr} ds$$

$$= \frac{x_{cr}}{NV} \sum_h \sum_k^{+\infty} |F^2_D| = x_{cr} \frac{|a \times b|}{V} 2\pi \int_0^\infty s \cdot [f^2] D ds \quad (5)$$

or

$$= \frac{x_{cr}}{NV} \sum_l^{+\infty} |F^2_D| = x_{cr} \frac{|c|}{V} 2 \int_0^\infty [f^2] D ds$$

$$[f^2] = \frac{1}{N} \left[ \sum_j f_j^2 + \sum_n \left( \sum_k f_k \right)^2 \right]. \quad (6)$$

$j$ : atoms which do not coincide in the projection on the  $ab$  plane along the direction of the  $c$ -axis or on the  $c$ -axis parallel to the  $ab$ -plane, respectively.

$k$ : atoms which coincide in these projections, forming  $n$  points of coincidence.

(Following Wilson, 1942).

$a, b, c$ : unit cell vectors.

It can be seen readily that in such cases some structural details are needed to evaluate the crystallinity, or more correctly, the amount of material which shows two- or one-dimensional order, whereas for three-dimensional order (interference peaks in all directions of the reciprocal space), the knowledge of the chemical composition is sufficient for the determination of  $x_{cr}$ .

To solve equation (4), the 'disorder' function  $D$  has to be determined. It is known that the oscillations of  $I(s)$  around  $\bar{f}^2$  are a function of the interatomic distances  $r_{jk}$  only,

$$I(s) = \bar{f}^2 + \frac{1}{\sum N_t} \sum_j \sum_{k \neq j} f_j f_k \frac{\sin 2\pi r_{jk} s}{2\pi r_{jk} s}. \quad (7)$$

For substances with the same chemical composition in the crystalline and the non-crystalline phases the smallest values of  $r_{jk}$ , which correspond to the chemical bond-lengths, rigid intramolecular distances and mean intermolecular distances, determine the long-

range fluctuation of these oscillations. Thus it should be possible to choose a number of integration intervals (limits  $s_o$  and  $s_p$ ) over larger regions of  $s$  such that

$$\int_{s_o}^{s_p} s^2 I(s) ds = \int_{s_o}^{s_p} s^2 \bar{f}^2 ds$$

independent of the crystallinity of the substance. These regions can be found experimentally by studying samples with different crystallinities.

We can then write equation (4) in the following form:

$$x_{cr} = \left\{ \int_{s_o}^{s_p} s^2 I_{cr}(s) ds \middle/ \int_{s_o}^{s_p} s^2 I(s) ds \right\} K(s_o, s_p, D, \bar{f}^2)$$

$$= \text{constant}$$

$$K = \int_{s_o}^{s_p} s^2 \bar{f}^2 ds \middle/ \int_{s_o}^{s_p} s^2 \bar{f}^2 D ds. \quad (8)$$

Having found a series of such regions, preferably with common lower limits  $s_o$ , we can solve the equation by determining the series of  $K$  values which yield  $x_{cr} = \text{constant}$  for a given  $D$ -function.

## Experimental

Four samples of polypropylene (prepared by J. Dale of these laboratories) and a commercial sample of polyethylene were chosen for the investigations:

Sample 1: Isotactic polypropylene heated to the melting point and quenched in water at room temperature.

Sample 2: The same, annealed 1 hr. at 105 °C.

Sample 3: The same, annealed  $\frac{1}{2}$  hr. at 160 °C.

Sample 4: 'Amorphous' polypropylene (heptane extract of crude polypropylene, highly atactic).

Sample 5: Polyethylene (low pressure).

Samples 1 to 4 were stacks of films, sample 5 a powder. No sample showed preferred orientation.

The X-ray scattering of these samples was measured at room temperature (20–25 °C.) with a Norelco counter diffractometer using a xenon-filled proportional counter and copper radiation. Monochromatization was carried out by using the Ross (1928) balanced filter method. The technique was similar to that described in a previous paper (Ruland, 1959). Angular dependence of the absorption corrections was eliminated by using thick samples ( $\exp[-2\mu t] \ll 1$ ) and appropriate relations between the apertures of primary beam and counter collimation systems. Line broadening due to the collimation conditions was not taken into account since only integrated intensities were to be investigated.

The scattering curves were constructed from several recordings in the regions 9–40°, 30–70° and 60–150° ( $2\theta$ ). The good proportionality obtained in the overlapping intervals confirmed that the experimental conditions had been suitably chosen. The  $\theta$ -scale was converted to the  $s$ -scale after correction for polarization.

All samples showed a continuous but not monotonic scattering at high values of  $s$ ; the diffraction peaks disappeared at  $s$ -values of about  $0.8 \text{ \AA}^{-1}$  for the polypropylene samples and about  $1.15 \text{ \AA}^{-1}$  for the polyethylene sample. Using equation (7) with only those  $r_{jk}$ -values which cannot be affected either by rotation within the chain molecule or by displacement of one molecule with respect to its neighbours, a scattering curve can be obtained which shows essentially the observed long-range oscillations at high values of  $s$  (see Fig. 1).

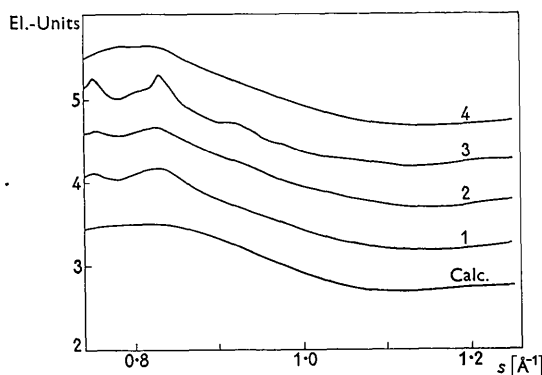


Fig. 1. High-angle scattering of polypropylene samples 1, 2, 3 and 4, and scattering curve calculated from the most rigid interatomic vector set.

The corresponding Compton scattering is given by:

$$I_{\text{incoh.}} = [\sum N_i I_i / \sum N_i] \cdot Q(s, \lambda).$$

$I_i$ : Compton scattering of an atom of type  $i$ .

$Q$ : Breit-Dirac recoil factor.

The scattering curve thus calculated could be fitted reasonably well to the experimental curves, but for higher  $s$ -values the theoretical curve was slightly higher than the experimental ones. This discrepancy can be explained by absorption effects, which change the ratio of Compton to coherent scattering due to the increasing difference of  $\lambda$  with increasing scattering angle. Under the given conditions there are four such effects, which can produce these discrepancies:

1. Absorption within the sample.
2. Absorption in the path from sample to counter.
3. Absorption by the balanced filters.
4. Absorption within the counter.

This leads to the following corrections:

1. For a flat sample in a counter diffractometer we find

$$I_{\text{coh.}} \propto \frac{1}{2\mu} \left[ 1 - \exp\left(-\frac{2\mu t}{\sin \theta}\right) \right].$$

$$I_{\text{incoh.}} \propto \frac{1}{2\mu + \Delta\mu} \left[ 1 - \exp\left(-\frac{(2\mu + \Delta\mu)t}{\sin \theta}\right) \right].$$

$\mu$ : linear absorption coefficient of the sample for the wavelength of the primary beam.

$\Delta\mu$ : difference between the linear absorption coefficients of the sample for the coherent and the Compton wavelengths.

$t$ : sample thickness.

If  $\exp(-2\mu t) \ll 1$  we find

$$(I_{\text{coh.}}/I_{\text{incoh.}})_{\text{obs.}} = (I_{\text{coh.}}/I_{\text{incoh.}})_{\text{th.}} \cdot (1 + \Delta\mu/2\mu).$$

obs.: observed.

th.: theoretical.

Since  $\mu$  is approximately proportional to  $\lambda^3$  outside the absorption edges, and  $\Delta\lambda$  is small compared with  $\lambda$ , we can write

$$\Delta\mu/2\mu = \frac{3}{2} \Delta\lambda/\lambda = (3h/mc\lambda) \sin^2 \theta = (\frac{3}{2} h\lambda/mc) s^2$$

provided there is no absorption edge between  $\lambda$  and  $(\lambda + \Delta\lambda)$  for any kind of atom in the sample.

For copper radiation we find a correction of about 5% for  $\theta_{\text{max.}}$ .

2. The absorption in air between sample and counter gives

$$(I_{\text{coh.}}/I_{\text{incoh.}})_{\text{obs.}} = (I_{\text{coh.}}/I_{\text{incoh.}})_{\text{th.}} \exp(\Delta\mu \cdot D).$$

$D$ : distance between sample and counter entry.

$\Delta\mu$ : difference of the linear absorption coefficients in air.

For  $D=20$  cm. we find about 2% for  $\theta_{\text{max.}}$ .

3. The intensity difference between two Ross filters of elements  $A$  and  $B$  is

$$\Delta I = I[\exp(-\mu_A t_A) - \exp(-\mu_B t_B)].$$

$t_A, t_B$ : thickness of filters  $A$  and  $B$ .

$\mu_A, \mu_B$ : linear absorption coefficients of elements  $A$  and  $B$ .

$I$ : unfiltered intensity of wavelength  $\lambda$ .

$t_A$  and  $t_B$  are chosen so that

$$t_B/t_A = \mu_A/\mu_B = q$$

for  $\mu_A$  and  $\mu_B$  outside the wavelength interval between the two absorption edges.

To obtain the maximum value of  $\Delta I$  for a given wavelength  $\lambda_0$  we find for  $(\partial \Delta I / \partial t_A)_{\lambda_0} = 0$

$$t_{A_0} = [\ln(q\mu_B) - \ln \mu_A] / [q\mu_B - \mu_A]$$

$$t_{B_0} = q t_{A_0}.$$

Using a filter set with these optimum thicknesses ( $t_0$ ), we find for small changes of  $\lambda$  around  $\lambda_0$ , since  $\mu$  is proportional to  $\lambda^n$  ( $n \approx 3$ ) and to  $t$ , so that  $\Delta I$  depends on  $\lambda$  and on  $t$  only through the function  $f = \lambda^n t$ :

$$(\partial \Delta I / \partial \lambda)_{t_0} = d\Delta I / df \cdot (\partial f / \partial \lambda)_{t_0} = 0$$

since

$$(\partial \Delta I / \partial t)_{\lambda_0} = (d\Delta I / df) \cdot (\partial f / \partial t)_{\lambda_0} = 0$$

which means  $d\Delta I / df = 0$ .

Thus in the case of a filter set with optimum thicknesses there is no appreciable change in  $\Delta I$  for

small  $\Delta\lambda$ , provided, of course, that the wavelength is not in the region of one of the absorption edges. Calculations showed that this is true for the maximum of  $\Delta\lambda$  measured with the filter set used for the experiments (Ni =  $6.8 \cdot 10^{-4}$  cm.; Co =  $7.55 \cdot 10^{-4}$  cm.). For thicknesses of  $10 \cdot 10^{-4}$  cm. Ni and  $11.1 \cdot 10^{-4}$  cm. Co we find a correction of about 3% for the maximum of  $\Delta\lambda$ .

4. For a detector with a quantum counting efficiency  $\eta$  which varies with  $\lambda$  we find

$$(I_{\text{coh.}}/I_{\text{incoh.}})_{\text{obs.}} = (I_{\text{coh.}}/I_{\text{incoh.}})_{\text{th.}} \cdot \eta/(\eta + \Delta\eta).$$

The proportional counter used in this work shows a flat maximum of  $\eta$  in the region of  $1.5 < \lambda < 2.0$  Å (Taylor & Parrish, 1955). The correction should therefore be negligible for copper radiation. If, however, molybdenum radiation had been used, there would be an error of about 10% for maximum  $\Delta\lambda$ . Similar effects are to be expected using film techniques.

In cases 1 and 2 the intensity of the Compton scattering is apparently smaller; in case 3 it is apparently greater for  $t < t_0$  and smaller for  $t > t_0$ , for  $t = t_0$  it has the right magnitude; in case 4 it can also appear greater or smaller according as the efficiency of the detector increases or decreases with wavelength.

For a thick sample ( $\exp(-2\mu t) \ll 1$ ) of general formula  $(\text{CH}_2)_n$  and for the experimental conditions of this work, these effects are shown in Fig. 2.

Application of these corrections to the theoretical scattering curve removed the discrepancies at high values of  $s$  and a satisfactory fit of the slopes of the

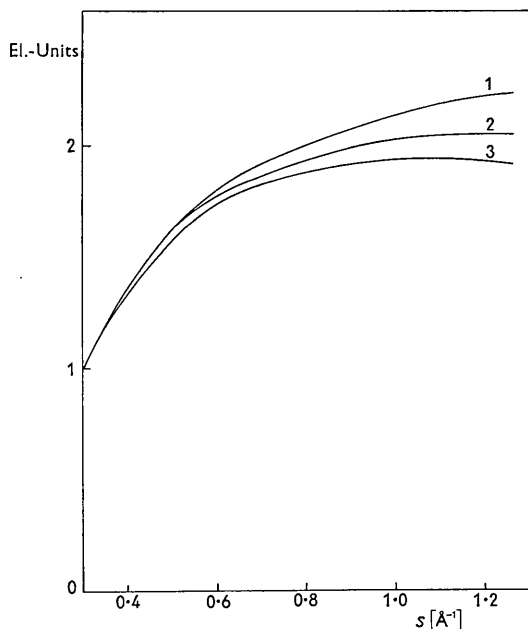


Fig. 2. Compton scattering calculated for  $(\text{CH}_2)_n$  in electron units per atom. 1. Uncorrected. 2. Breit-Dirac factor applied. 3. Breit-Dirac factor and absorption correction applied.

experimental and theoretical curves was obtained. Thus the normalization could be performed for the whole of the scattering and the separation of the Compton scattering became possible.

The atomic scattering factors used were those given by Berghuis *et al.* (1955) for carbon in the valence state, by Keating & Vineyard (1956) for the Compton scattering of carbon and by McWeeny (1951) for hydrogen. The scattering functions were subtabulated at intervals of  $s=0.01$  by the method of bridging differences (Hartree, 1952).

The next step was the choice of independent regions of crystallinity for use in equation (8). These could be found easily by trial in the case of the series of polypropylene samples using a planimeter and an  $s^2I(s)$  plot. For polyethylene similar regions were chosen. Comparison of the integrals in  $s^2I(s)$  with those in  $s^2\bar{f}^2$  showed that the calculated  $\bar{f}^2$  values represent the structure-independent scattering (see equation (7)) reasonably well for  $s$ -values greater than 0.4. For lower values of  $s$  these  $\bar{f}^2$  values are about 30% too small. A thorough check of the experimental conditions, especially with respect to multiple scattering (Warren, 1959), showed that no error of this magnitude could have been introduced by them. Similar studies on organic compounds with carbon-hydrogen atomic ratios above unity showed that the atomic scattering factors used represent satisfactorily the structure-independent scattering. In view of these facts it is very likely that the discrepancies found in this work are due to the C-H bond orbitals which cannot be represented by spherically symmetrical electron-density distributions in the carbon and hydrogen atoms such as was assumed in the calculation of  $\bar{f}^2$ . It should be mentioned that Bunn (1939) found similar discrepancies in comparing observed and calculated structure factors for polythene.

Inspection of equations (4) and (8) shows, however, that these discrepancies cannot influence the results very much since in both fractions numerator and denominator behave similarly as functions of the upper limit of the integration and also because the deviation of  $\bar{f}^2$  from its experimental values is restricted to small values of  $s$  where the  $D$ -function is close to unity.

The separation lines between the crystalline peaks and continuous scattering have been established by drawing smooth curves from tail to tail following the general slope of the continuous scattering. By doing so we restrict the designation 'crystalline' to crystalline regions larger than 20-30 Å, and containing lattice imperfections of the second kind not exceeding r.m.s. deviations of about 10% in the nearest neighbour distances.

The separation procedure is less critical in this method than in the usual crystallinity methods because of the number of peaks used, which in this work was up to 25, whereas in the usual methods

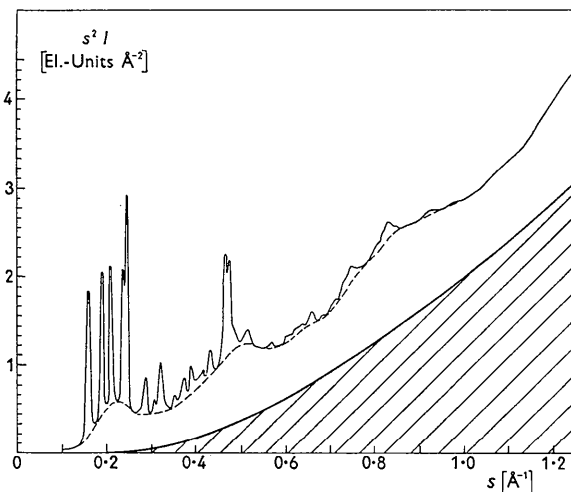
Table 1. Crystallinity (weight fraction  $x_{cr}$ ) as function of  $k$  and integration interval

Polypropylene								
Interval	Sample 1		Sample 2		Sample 3		Sample 4	
	$k=0$	$k=4$	$k=0$	$k=4$	$k=0$	$k=4$	$k=0$	$k=4$
$s_o - s_p$	0.270	0.329	0.353	0.431	0.546	0.666	0.120	0.146
0.1-0.3	0.159	0.294	0.222	0.411	0.333	0.616	0.078	0.144
0.1-0.6	0.105	0.305	0.145	0.421	0.220	0.638	0.044	0.128
0.1-0.9	0.067	0.315	0.095	0.447	0.145	0.682	0.029	0.136
0.1-1.25		0.31		0.43		0.65		0.14
$x_{cr}$								

Polyethylene		
Interval	Sample 5	
	$k=0$	$k=2$
$s_o - s_p$	0.494	0.563
0.1-0.35	0.354	0.538
0.1-0.70	0.276	0.542
0.1-0.95	0.200	0.552
0.1-1.25		0.55
$\bar{x}_{cr}$		

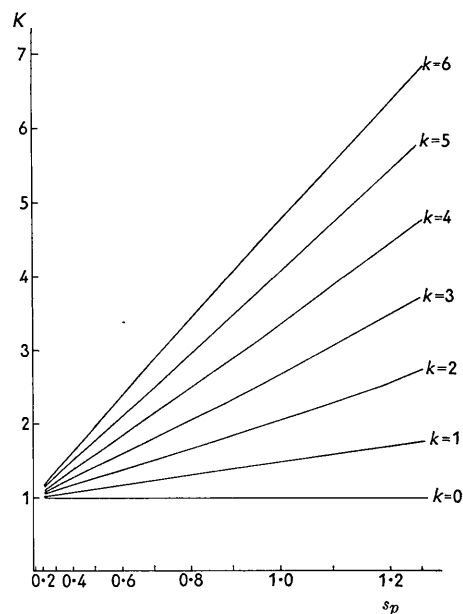
only a few peaks are considered. An example is shown in Fig. 3.

Fig. 3.  $s^2 I(s)$ -curve of polypropylene (sample 3).

The results of the application of equation (8) with  $D$  taken as  $\exp(-ks^2)$  are shown in Table 1.

It can be seen that by taking  $k=4$  for the polypropylene samples and  $k=2$  for the polyethylene sample, fairly constant values are obtained from different regions of integration. There is a trend towards smaller values in the medium regions, which may indicate that the disorder effects are not isotropic and a better fitting  $D$ -function would be a series of gaussian curves, but since the deviations in  $x_{cr}$  are not so significant, an isotropic  $D$ -function can be regarded as a good approximation.

Fig. 4 shows a nomogram of the  $K$ -values for  $s_o=0.1$ , which give fairly straight lines for  $k=\text{constant}$  when plotted against  $s^2$ . This empirical relationship can be used to determine  $k$  graphically.

Fig. 4. Nomogram of  $K$ -values as function of  $k$  and  $s_p$ ,  $s_o=0.1$ .

## Discussion

The values given in Table 1 show that it is necessary to take into account the effect of thermal vibrations and disorder phenomena in crystallinity determinations. They show also that the 'disorder' function can be determined together with the crystallinity without having more information on the substance than its chemical constitution. An interesting fact is that the 'disorder' function determined for the four polypropylene samples is exactly the same, despite their different thermal histories. This seems to indicate that the effect of lattice imperfections is small compared with that of the thermal vibrations because it could be expected that the former are influenced by quenching and annealing.

In recent work on crystal-structure determination of polypropylene by Natta & Corradini (1960) an isotropic temperature factor with a  $B$ -value of  $7.5-8.5 \text{ \AA}^{-2}$  had been found, which is in close correlation to  $k=B/2=4 \text{ \AA}^{-2}$  found in this work, confirming the above statement.

These results are in favour of a two-phase system of crystalline and non-crystalline regions. The crystalline parts should be well ordered and gradual transitions from this structure to the structure of the non-crystalline parts cannot be present in appreciable amounts, since such intermediate structures should not only contribute to the crystallinity but also to the 'disorder' function. It is difficult to obtain any information on the structure of the non-crystalline part by X-ray studies alone, because there is no possibility of separating the diffuse scattering due to this part from that due to thermal vibrations of the crystalline part by working at room temperature only. Other methods may help here to give further information.

Infrared studies have been carried out by Dale (1959) on the four samples of polypropylene investigated in this work. It has been found that there are some absorption bands in the spectrum of the solid isotactic polymer which disappear in the spectrum of the molten isotactic material; in highly atactic solid samples these bands have been absent or very weak. From this it was concluded that these absorption bands are due to special chain conformations, characteristic for the crystalline state, and the absence of these bands should indicate random-coil formation. Quantitative determination of the amount of material which produces these bands had been carried out on the four samples in question. The conclusion was that the isotactic samples whether quenched or annealed should consist almost completely of such material, whereas the highly atactic sample contained a fraction which was of the same order of magnitude as the X-ray crystallinity. The non-crystalline part of the isotactic samples should thus show a preformation of the crystalline arrangement, a 'paracrystalline' state of a higher degree of disorder than can be assessed by the X-ray method, but, as has been pointed out above, cannot contain structures of degrees of disorder intermediate between this 'paracrystalline' state and the crystalline state.

The absence of such structures seems to be reasonable since slightly disturbed intermolecular arrange-

ments will be unstable already at room temperature if they are fixed by Van der Waals forces only. This will not be the case for intermolecular arrangements fixed e.g. by hydrogen bonds.

This work is part of a project sponsored by the Union Carbide Corporation, New York, and I take this opportunity to express my appreciation of this support.

I am indebted to Drs H. Tompa, P. B. Hirsch and R. Hosemann for helpful advice during the course of this work and to Drs B. Hargitay, J. Dale, V. Sandor and J. F. M. Oth for general discussions of the problem of crystallinity.

My thanks are also due to Mr J. P. Pauwels and to the staff of the IBM installation in this laboratory for carrying out the calculations.

### References

- AGGARWAL, S. L. & TILLEY, G. P. (1955). *J. Polym. Sci.* **18**, 17.
- BERGHUIS, J., HAANAPPEL, IJ. M., POTTERTS, M., LOOPSTRA, B. O., MACGILLAVRY, C. H. & VEENENDAAL, A. L. (1955). *Acta Cryst.* **8**, 478.
- BUNN, C. W. (1939). *Trans. Farad. Soc.* **35**, 482.
- DALE, J. (1959). Private communication.
- GOPPEL, J. M. & ARLMANN, I. J. (1949). *Appl. Sci. Res.* **A1**, 462.
- HARTREE, D. R. (1952). *Numerical Analysis*. Oxford: Clarendon Press.
- HERMANS, P. H. & WEIDINGER, A. (1950). *J. Polym. Sci.* **5**, 565.
- HOSEMAN, R. (1950a). *Z. Phys.* **128**, 1.
- HOSEMAN, R. (1950b). *Z. Phys.* **128**, 465.
- HOSEMAN, R. (1951). *Acta Cryst.* **4**, 520.
- HOSEMAN, R. (1960). *Norelco Rep.* **7**, 81.
- KARTHA, G. (1953). *Acta Cryst.* **6**, 817.
- KAST, W. & FLASCHNER, L. (1948). *Kolloidzshr.* **111**, 6.
- KEATING, D. T. & VINEYARD, G. H. (1956). *Acta Cryst.* **9**, 895.
- KRIMM, S. & TOBOLSKY, A. V. (1951). *J. Polym. Sci.* **7**, 57.
- MCWEENY, R. (1951). *Acta Cryst.* **4**, 513.
- MATTHEWS, J. L., PEISER, H. S. & RICHARDS, R. B. (1949). *Acta Cryst.* **2**, 85.
- NATTA, G. & CORRADINI, P. (1960). *Nuovo Cim. Suppl.* **15**, 40.
- NORMAN, N. (1957). *Acta Cryst.* **10**, 370.
- ROSS, P. A. (1928). *J. Opt. Soc. Amer.* **16**, 433.
- RULAND, W. (1959). *Acta Cryst.* **12**, 679.
- TAYLOR, T. & PARRISH, W. (1955). *Rev. Sci. Instrum.* **26**, 367.
- WARREN, B. E. (1959). *J. Appl. Phys.* **30**, 1111.
- WILSON, A. J. C. (1942). *Nature, Lond.* **150**, 151.